Catalysis Science & Technology

ROYAL SOCIETY OF CHEMISTRY

COMMUNICATION

View Article Online
View Journal

Cite this: DOI: 10.1039/d6cy00118a

Received 30th January 2026,
Accepted 10th March 2026

DOI: 10.1039/d6cy00118a

rsc.li/catalysis

Continuous-flow hydroprocessing of long-chain fatty acids: reaction pathways and the impact of lignin-derived aromatics towards efficient deoxygenation

Rita Assis dos Santos, *[ab] Arij Ben Hassine,[b] Pedro José Sanches Filho,[b] M. Joana Neiva Correia [ac] and Pedro S. F. Mendes *[ab]

This study has established oleic acid reaction pathways under long-term continuous-flow hydroprocessing, highlighting the roles of metal and acid sites for efficient deoxygenation. At industrially relevant conversions, guaiacol co-feeding, despite accelerating catalyst deactivation, largely preserved the oleic-acid–derived fingerprint (83 wt% of the organic fraction) with mixed-origin products accounting for the remainder. These findings allow tailoring sustainable aviation fuel composition while diversifying non-conventional feedstocks.

Introduction

Achieving carbon neutrality, important for slowing down climate change, remains an open challenge in the aviation sector. Aircraft require high–energy-density and intrinsically safe fuels, properties that are currently delivered by liquid hydrocarbons (HC), but that are not likely to be done so in the near future by batteries or gas fuels (*e.g.*, hydrogen).[1–3] Sustainable aviation fuels (SAFs), derived from renewable or waste-based sources, are therefore key routes to reducing the global warming footprint of aircraft.[1,3–6] SAFs have a chemical composition similar to that of conventional jet fuel (including iso-paraffins, paraffins, aromatics and cycloalkanes), making them compatible with existing infrastructure.[3,4] Despite strong policy support (*e.g.*, ReFuelEU, which targets 6% and 20% levels of SAF incorporation by 2030 and 2035, respectively[1]), global SAF production remains limited and below expectations.[1,2,4]

Of the approved production routes, hydroprocessed esters and fatty acids (HEFA) is currently the most technologically mature and commercially deployed process.[1–4,6] HEFA converts mainly lipidic feedstocks, such as vegetable oils, animal fats, or used cooking oils, into HC through deoxygenation (primarily acid-catalysed[7] hydrodeoxygenation (HDO) and metal-catalysed[7,8] decarboxylation (DCO_x) and decarbonylation (DCO)), followed by acid-catalysed[7,9] hydrocracking (HCK) and hydroisomerisation (HDI) reactions.[4–6,10]†

The scalability of HEFA fuels is nevertheless constrained by the limited global availability and cost of lipidic feedstocks,[1,2,5,6] motivating research towards incorporating more abundant resources, such as lignocellulosic biomass.[2,3,6,10] The simultaneous hydroprocessing of lipidic and lignocellulosic-derived feedstocks, potentially in existing refinery units, is thus a promising strategy.[10] This integrated approach not only diversifies feedstock supply chains and potentially reduces costs but also enables tuning of paraffinic and aromatics fractions to meet jet fuel specifications, including cold flow and aromatic content requirements.[1,10]

Nonetheless, lipidic and lignocellulosic-derived feedstocks differ significantly in chemical structure, being long-chain fatty acids and oxygen-containing aromatic compounds, respectively. These differences may result in unexpected interactions when processed together. In other words, mixture effects impacting, *e.g.*, deoxygenation efficiency or product selectivity, may arise under simultaneous hydroprocessing.[11]

While the individual hydroprocessing of representative model compounds, such as oleic acid and guaiacol, has been studied often in batch systems,[7,12–17] and less commonly in continuous-flow,[18–21] mixture effects are yet to be established. Batch conversion blends of bio-oil and waste/vegetable oils over acidic (Ni)CoMo catalysts (mainly used for investigating fuel yields, coke formation and solvent effects) have shown that lignin-derived compounds influence coke formation and overall product distribution.[22,23] Under continuous operation over non-acidic (Ni)CoMo catalysts, mixtures of mono-substituted oxygen-containing aromatics with, respectively,

[a] *Departamento de Engenharia Química, Instituto Superior Técnico, Universidade de Lisboa, Av. Rovisco Pais, 1049-001 Lisboa, Portugal.*
E-mail: rita.assis.santos@tecnico.ulisboa.pt, pedro.f.mendes@tecnico.ulisboa.pt
[b] *Centro de Química Estrutural, Institute of Molecular Sciences, Instituto Superior Técnico, Universidade de Lisboa, Av. Rovisco Pais, 1049-001 Lisboa, Portugal*
[c] *Centro de Recursos Naturais e Ambiente, Instituto Superior Técnico, Universidade de Lisboa, Av. Rovisco Pais, 1049-001 Lisboa, Portugal*

short-chain carboxylic acids and aldehydes exhibited shifts in conversion (with different magnitudes) to higher temperatures due to competitive adsorption, with carboxylic acids exerting the stronger impact on the conversion of other compounds.[19] Similarly, studies on lauric acid/anisole and indole-containing mixtures over acidic and non-acidic nickel-based catalysts (*e.g.*, NiMo) demonstrated the suppression of C–O cleavage of anisole until other reactants were consumed. This suppression led to reduced yields of deoxygenated HC in the presence of carboxylic acids or nitrogen-containing compounds.[11,24] Furthermore, in lauric acid/indole mixtures, there was an increase in the production of condensation products.[11] Additionally, multiscale and microkinetic modelling approaches have been applied to analyse reaction mechanisms and transport phenomena in hydroprocessing systems for various compound families.[25,26] Collectively, these studies have demonstrated that co-feeding chemically distinct compounds can modify conversion behaviour and induce competition or inhibitory effects between feedstocks. However, products are often analysed as bulk HC lumps, hindering a comprehensive analysis of the underlying reaction pathways. Consequently, an understanding of how mixture effects influence deoxygenation routes under continuous operation remains limited.

The objective of this work is therefore to evaluate potential mixture effects arising from the simultaneous hydroprocessing of chemically distinct model compounds, by carrying out experiments leading to an understanding of individual reaction pathways under industrially relevant (*i.e.*, continuous, high conversion) operation. First, the conversion-controlled reaction pathways for oleic acid were established by carrying out a long-duration experiment (time on stream (TOS) >72 h, as defined in SI section 1.3) under fixed operating conditions (T = 360 °C, P = 40 bar, H_2/oleic acid = 1000 NmL mL^{-1}, weight hourly space velocity (WHSV) = 9.4 h^{-1}) and catalyst formulation (reference bifunctional 20Ni/HZSM-5 catalyst). The results of this experiment then served as a basis for investigating mixture effects in simultaneous hydroprocessing with guaiacol, *via* the impact of the oxygen-containing aromatic on fatty acid‡ conversion and organic product distribution under continuous operation.

Oleic acid single-feed experiment

To establish a comprehensive pathway scheme of the cascade reactions, (i) conversion was followed over an extended TOS to capture key intermediates and products, and (ii) a bifunctional catalyst was selected to investigate the metal and acid functions. Moreover, to ensure intrinsically reproducible results, the catalyst was prepared by mechanical mixing of two commercially available materials (vide detailed procedures in SI section 1.2). Details on feedstocks, catalyst preparation and characterisation, experimental setup, product analysis, and data treatment are provided in SI section 1.

Reaction pathways

The reaction pathways were determined by combining product distributions (over different conversions) with stoichiometric analysis based on molar flow rates (vide SI, section 2.2) and ultimately validated against individual pathways reported in the literature (vide SI, section 2.1). Therefore, all the reaction pathways were determined based on experimental data, but with the active sites primarily catalysing each reaction determined exclusively by literature, and hence not presented here (vide SI, Table S3). Although not the focus of this study, primary reaction mechanisms, when available, are also disclosed in SI section 2.1, based on literature.

The proposed reaction network for oleic acid hydroprocessing over a bifunctional catalyst is presented in Fig. 1. Its description follows the progression of the cascade reactions through key oxygen-containing intermediates, ultimately culminating in deoxygenated HC. Note that according to the evidence collected from various experiments (vide SI, Fig. S11), catalyst deactivation over time does not in a major way affect the reaction pathways discussed hereafter, as it mainly leads to the suppression of hydrogenolysis and HCK (further discussion in SI section 2.3).

Initial hydrogenation of unsaturated fatty acids was identified as a major (vide SI, Fig. S8) and relatively fast step,[7,27,28] with this description consistent with energetic considerations due to the enthalpy required for C=C hydrogenation (614 kJ mol^{-1}) being lower than that for the C=O bond cleavage (799 kJ mol^{-1}).[14] Linoleic acid was first hydrogenated to oleic acid and subsequently to stearic acid (reactions 1–2 in Fig. 1), considering that its relative abundance decreased from 22 wt%§ to 0.3 wt% upon conversion increase (vide SI, Fig. S8). Note the formation of stearic acid (<25 wt%), establishes a central saturated fatty acid from which subsequent oxygen-containing species can be generated—with these species, at lower conversions (<90 wt%), including octadecanol, octadecanal, stearyl stearate and dioctadecyl ether (vide SI, Fig. S8), which can possibly be further converted.

Low ester amounts (<8 wt%) were detected experimentally (vide SI, Fig. S8), indicating esterification between stearic acid and octadecanol (reaction 3 in Fig. 1)[25,27,29] to be a minor route, bridging key fatty-acid and alcohol intermediates within the reaction network. Nevertheless, esters have been reported in the literature to be reactive under hydroprocessing conditions and may undergo further transformations, such as dehydration to octadecene.[8,27] Etherification proceeded *via* dehydration of octadecanol molecules (reaction 4 in Fig. 1, right-hand side), forming low dioctadecyl ether amounts (<1 wt%) and water.[25,30] Their relative abundance decreased with increasing conversion (vide SI, Fig. S8), indicating that ether formation is a minor route rather than a key intermediate step. In general, compared to esters, ethers are less reactive and are thus less likely to undergo further reactions.

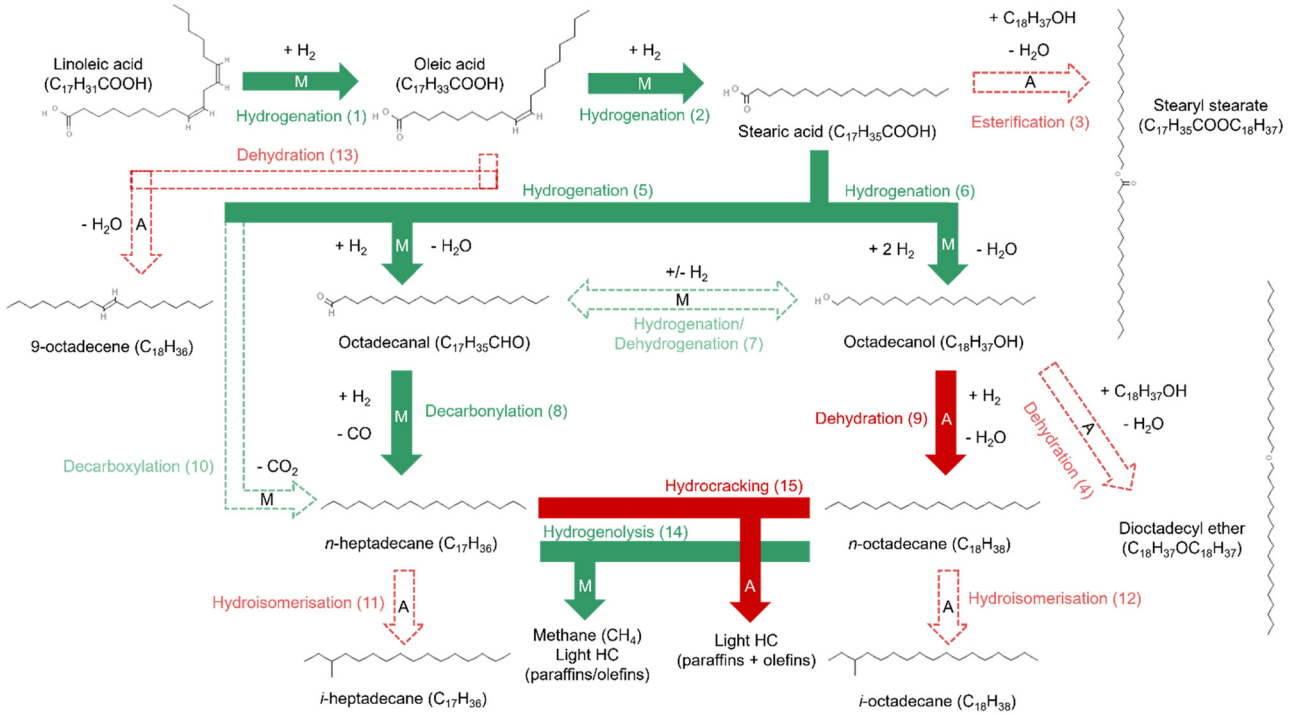

Fig. 1 Proposed reaction pathways for oleic acid hydroprocessing over 20Ni/HZSM-5. Green arrows represent reactions primarily catalysed by metal sites (M), while red arrows represent reactions primarily catalysed by acid sites (A). Solid arrows correspond to major pathways, whereas dashed, lighter-coloured arrows correspond to minor pathways. Reaction pathways were experimentally determined, with active sites based exclusively on literature (vide SI, Table S3).

Octadecanal and octadecanol (<1 wt%) can be produced from hydrogenation of stearic acid (reactions 5–6 in Fig. 1) and subsequently interconvert through hydrogenation/dehydrogenation (reaction 7 in Fig. 1),[7,8,25,29] forming a central reaction node from which two major deoxygenation routes subsequently emerge. Octadecanal can undergo DCO to yield the corresponding C_{17} HC (>30 wt%) (reaction 8 in Fig. 1),[7,27,28] while octadecanol can be dehydrated to produce the corresponding C_{18} HC (>10 wt%) (reaction 9 in Fig. 1).[7,28] In addition to these pathways, stearic acid can be directly converted to heptadecane *via* DCO_x (reaction 10 in Fig. 1).[7] This route was identified as minor based on gaseous product analysis, where CO_2 amounts never exceeded 5 wt% of the gaseous products (vide SI, Fig. S10), consistent with previous studies.[31] Both C_{17} and C_{18} HC can subsequently undergo HDI (reactions 11–12 in Fig. 1),[7,27] though this reaction remained limited, given the low isomer to HC ratios for both compounds (*ca.* 0.1, vide SI, Fig. S12).

Interestingly, our results suggest possible direct dehydration of oleic acid to octadecene (reaction 13 in Fig. 1)[27] without prior hydrogenation (vide SI, section 2.3). Hydrogenolysis and HCK (reactions 14–15 in Fig. 1) represent additional important pathways.[7,12,13,27,28] In hydrogenolysis, either paraffins or olefins can be produced depending on H_2 availability, though under hydroprocessing conditions olefins tend to hydrogenate back to paraffins.[32] Cracking products may also include paraffin-paraffin or paraffin-olefin pairs. These smaller fragments may further recombine,[7] accounting for the formation of HC with carbon chains larger than C_{18} HC, at most 13 wt% (not depicted in Fig. 1, vide SI and S9).

Role of active sites in the reaction pathways

The network proposed here integrates these individual reactions into a unified cascade, capturing both major and minor pathways, over a representative bifunctional catalyst. As many of these reactions have been studied in detail separately (vide SI, Table S3 and section 2.1), this active-site–specific knowledge from literature was leveraged to specify the roles of metal and acid sites in the overall deoxygenation network (see text inside arrows in Fig. 1).

Under the studied conditions, the results pointed towards a reaction network governed by metal-catalysed pathways. The HC fraction consistently exhibited a predominance of C_{17} HC (>60 wt%) (vide SI, Fig. S9), and CO/CO_2 were detected in the gas phase (vide SI, Fig. S10), indicating that metal-catalysed DCO/DCO_x prevailed over acid-catalysed HDO. This behaviour aligns with a previous single-feed batch study using analogous catalysts and feedstocks, where metal-site–dominated systems favoured alkane formation.[27] Furthermore, other studies also reported nickel-based catalysts and high temperatures (particularly 375 °C[14]) promoting DCO/DCO_x over HDO.[12,28] The selectivity towards metal-catalysed reactions, despite the presence of strong Brønsted acidity in ZSM-5, can be tentatively attributed

to the high metal loading and limited accessibility of Brønsted acid sites, considering the larger kinetic diameter of oleic acid (8 Å[33]) relative to the ZSM-5 pore diameter (5.1–5.6 Å[34]).

Guaiacol co-feeding experiment

To isolate the specific impact of guaiacol co-feeding, *i.e.*, without introducing additional variables, the catalyst formulation and operating conditions used in the conversion-controlled oleic acid single-feed experiment (described above) were also used here. In particular, the oleic acid partial pressure at the reactor inlet was preserved by replacing part of the excess H_2 with guaiacol, thereby avoiding spurious effects in the reaction rates. An 87/13 oleic acid/guaiacol mass ratio was selected to reflect industrially relevant SAF blending targets (6% and 20% by 2030 and 2035, respectively, according to ReFuelEU[1]) while ensuring sufficient product concentration for reliable quantification.

Feedstock conversion

Feedstock conversion profiles‡ are presented in Fig. 2. Fatty acid conversion was consistently lower in the presence of guaiacol than in the single-feed experiment. This effect was accompanied by a more pronounced relative abundance of stearic acid (vide SI, Fig. S14a), indicating a lower overall reaction progression under simultaneous hydroprocessing. Guaiacol itself exhibited conversions below 70% over the 72 h period, lower than those of the fatty acids. Notably, both fatty acids and guaiacol conversions declined by approximately 40% (from 91% to 51% and from 67% to 39%, respectively) during simultaneous hydroprocessing, with these declines roughly twice that observed for fatty acids under single-feed conditions (from 99% to 83%).

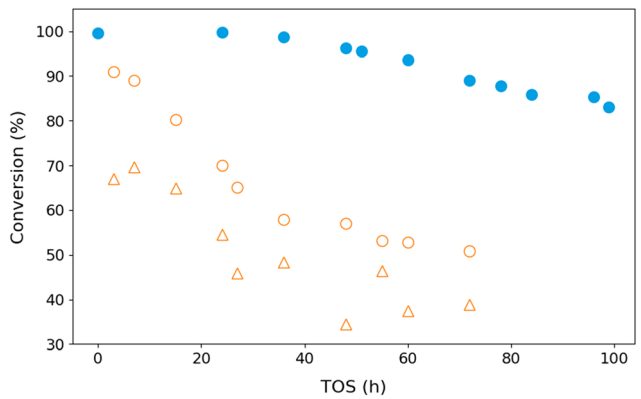

Fig. 2 Fatty acid and guaiacol conversion for single-feed (oleic acid) and simultaneous hydroprocessing (oleic acid/guaiacol mixture, 87/13 mass ratio) experiments over 20Ni/HZSM-5 (P = 40 bar, T = 360 °C, H_2/oleic acid = 1000 NmL mL^{-1}, WHSV = 9.4 h^{-1}). Single-feed experiment: fatty acid conversion (●); simultaneous hydroprocessing: fatty acid conversion (○), guaiacol conversion (△). Fatty acid conversion includes contributions from linoleic, oleic and stearic acids.

Concerning the initial fatty acid conversion (*i.e.*, at TOS approaching zero), the evidence was limited to the first sampling point and included a certain time lag. Still, fatty acid conversion seemed to be lower in simultaneous hydroprocessing than in the single-feed experiment, suggestive of competitive adsorption between oleic acid and guaiacol for active sites. Both oleic acid and guaiacol hydroprocessing pathways require metal and acid sites for efficient deoxygenation (vide Reaction pathways section). Although several guaiacol reactions are acid-catalysed, they also involve the metal function to promote deoxygenation[16,35,36]—meaning that strong adsorption of guaiacol onto the catalyst surface[21] could hinder fatty acid conversion. Although over simpler model compounds (anisole and heptanoic acid), a previous study has also shown that co-feeding carboxylic acids and aromatic compounds shifts conversion to higher temperatures due to the competitive adsorption of both molecules on active sites.[19] Concerning deactivation, plots of conversion *versus* TOS (Fig. 2) show two distinct deactivation profiles for the single-feed (blue filled markers) and simultaneous hydroprocessing (orange unfilled markers), respectively. In the plot for the single-feed experiment, an S-shaped curve, with an initial induction period with limited impact, followed by a sharp increase in the slope, was observed, indicating a cumulative or sequential effect.[37] In contrast, during simultaneous hydroprocessing, the conversion immediately dropped, *i.e.*, from low TOS, with the slope progressively decreasing over time, in an exponential-decay–like fashion. This accelerated and more severe deactivation observed in the presence of guaiacol pointed to its potential role as a deactivation precursor. Polymerisation of unsaturated phenolic compounds such as guaiacol is considered one of the main causes for coke formation in hydroprocessing, through the production of condensed polyaromatic species.[22,23,35,38] Other continuous-flow studies using oxygen-containing aromatics and nickel-based catalysts also reported fast catalyst deactivation (within the first 5 h).[39] On the other hand, fatty acids alone are not considered primary coke precursors and typically require the prior formation of by-products.[38]

In summary, based on the feedstock conversion profiles, guaiacol co-feeding led to overall lower fatty acid conversion along with a faster and more severe catalyst deactivation, compared with the single-feed oleic acid experiment.

Organic product distribution

To further elucidate mixture effects in terms of preferred reaction pathways, organic product distributions of oleic-acid–derived products were determined at iso-conversion under high (*ca.* 90%) and moderate (*ca.* 50%) conversion levels, as depicted in Fig. 3a and b, respectively. Different conversion levels were achieved by following the evolution with TOS under otherwise identical conditions or by varying WHSV. To prevent any interference of guaiacol-derived products, the distribution analysis focused on C_8+ HC products. This focus also limited the influence of catalyst deactivation on

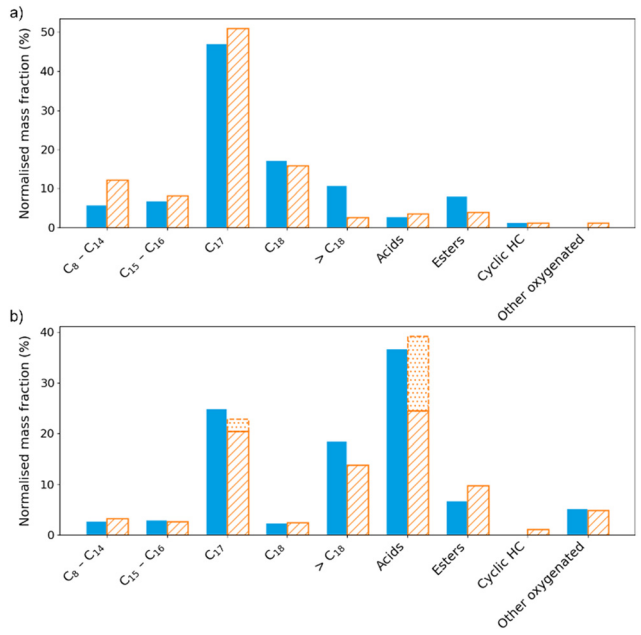

Fig. 3 Product distribution evolution in the organic phase for single-feed (oleic acid) and simultaneous hydroprocessing (oleic acid/guaiacol mixture, 87/13 mass ratio) experiments over 20Ni/HZSM-5 (excluding linoleic, oleic and stearic acids): a) high conversion (*ca.* 90%); b) moderate conversion (*ca.* 50%). Single-feed: oleic-acid–derived products (▬); simultaneous hydroprocessing: oleic-acid–derived products (▨); estimated mixed-origin products, namely phenolic esters and aliphatic ketones (⬚). Common operating conditions: P = 40 bar, T = 360 °C, H_2/oleic acid = 1000 NmL mL^{-1}. High conversion conditions: WHSV = 9.4 h^{-1}; single-feed at TOS = 60 h; simultaneous hydroprocessing at TOS = 3 h. Low conversion conditions: single-feed at WHSV = 19.0 h^{-1} and TOS = ~ 14 h; simultaneous hydroprocessing at WHSV = 9.4 h^{-1} and TOS = 72 h.

the observed products (and pathways), due to the key differences here being chiefly C_7− HC (formed *via* hydrogenolysis and HCK, vide SI, section 2.3). High conversion conditions are discussed first, allowing for a direct comparison of oleic-acid–derived products without interference from mixed-origin condensation products, which were only observable at lower conversions.

Regarding the case of high conversion (Fig. 3a), the overall product distributions observed under single-feed and simultaneous hydroprocessing conditions were remarkably similar (the minor variations were deemed rather negligible when accounting for experimental uncertainty). This observation demonstrated the robustness of oleic acid reaction pathways even in the presence of oxygen-containing aromatics. For the moderate conversion scenario (Fig. 3b), a similar overall fingerprint was observed, with apparent differences in the carboxylic acid fraction (represented by striped bars). Under these conditions, mixed-origin products (namely phenolic esters and aliphatic ketones) were detected (vide SI, section 3), whereas they were absent at high conversion, making up the largest contribution to the difference between the product distributions, namely in the acids and C_{17} HC fractions (represented by the dotted bars).

Overall, these results indicated that although catalyst deactivation strongly influences conversion levels, it does not significantly affect the oleic-acid–derived product distribution (over the studied operating conditions). This conclusion is consistent with single-feed observations (vide SI, Fig. S11) of deactivation having primarily suppressed hydrogenolysis and HCK reactions, a classical effect in HC hydroprocessing.[9,32] Since the light-HC fractions associated with these pathways were comparable in both the high- and moderate-conversion experiments (Fig. 3(a and b)), the differences observed may be concluded to be governed by conversion levels rather than by catalyst deactivation.

Therefore, over this representative bifunctional catalyst and at these conversion levels, the primary mixture effect at the product level when co-feeding guaiacol is the formation of mixed-origin products, rather than a fundamental change in oleic acid reaction pathways.

Oleic acid co-feed reaction pathways

Taking the results of the previous section into account, the proposed network can be further validated at moderate conversions. At such conversions, the product distribution was dominated by oxygen-containing intermediates, particularly stearic acid, a key intermediate in oleic acid hydroprocessing. As conversion increased, the cascade reactions (presented in Fig. 1) leading to deoxygenated HC were favoured, resulting in higher HC yields and lower acid ones. This trend illustrated how the progression through the cascade reactions drives the system from oxygen-containing species towards fully deoxygenated products.

Despite these conversion-dependent changes, the HC fraction consistently exhibited a predominance of C_{17} HC (vide SI, Fig. S14a), indicating that metal-catalysed DCO/DCO$_x$ were the major hydroprocessing pathways, rather than acid-catalysed HDO, which is consistent with the single-feed experiment (vide role of active sites in the reaction pathways section). As shown in Fig. 3, the formation of mixed-origin products was also observed at lower conversions (*ca.* 50%), providing additional insights into the chemical reactivity between oleic acid and guaiacol. To the best of our knowledge, the formation of these mixed-origin species has not been previously reported. To further understand these results, tentative reaction pathways were proposed (vide SI, Fig. S15), specifically inferred from the relative abundance of the reactants, as well as the molecular structures of potential reactants and their textbook functional group reactivities. According to this proposal, the phenolic esters (the main mixed-origin products (15 wt%)) are likely formed *via* esterification reactions, which would require a carboxylic group and an alcohol function.[40] Here, the guaiacol hydroxyl group provides the alcohol function, while oleic acid supplies the carboxylic acid functional group. The aliphatic ketones (2 wt%) may result from coupling reactions between ketones and olefins.[41] Cyclohexanone (formed during guaiacol hydroprocessing) reacts with unsaturated HC such as heptadecene (generated from oleic acid

hydroprocessing), which offers reactive sites for C–C bond formation with the cyclohexanone structure.

Conclusions

Under the studied operating conditions in long-term hydroprocessing over a representative bifunctional catalyst (20Ni/HZSM-5), oleic acid's cascade reactions were initiated by rapid hydrogenation to stearic acid, considering that its relative abundance decreased as fatty acid conversion increased. This hydrogenation was followed by metal-catalysed decarbonylation to C_{17} HC, the predominant product (>30 wt% of the organic fraction), and acid-catalysed dehydration to C_{18} HC (> 10 wt% of the organic fraction). During simultaneous hydroprocessing with guaiacol, despite accelerated catalyst deactivation evidenced by a distinct conversion profile, the oleic-acid–derived fingerprint (83 wt% of the organic fraction) was largely preserved over a wide conversion range (*ca.* 50–90%), demonstrating the robustness of oleic acid reaction pathways even in the presence of oxygen-containing aromatics. At lower conversion levels (*ca.* 50%), mixture effects were primarily reflected in the moderate formation of mixed-origin products (17 wt% of the organic fraction), such as phenolic esters and aliphatic ketones, rather than in changes in HC selectivity. In summary, oleic acid hydroprocessing resulted in efficient deoxygenation through a predominantly metal-site–dominated reaction network. The experimental data, despite being limited to the catalyst selected and operating conditions covered, allowed us to assess simultaneously both metal and acid sites over a rather wide conversion range (*ca.* 50–99%), increasing the potential of generalising the reaction network to other continuous systems. These findings highlight the potential of simultaneous processing strategies to diversify feedstocks while controlling sustainable aviation fuel composition.

Author contributions

Rita Assis dos Santos: conceptualization, data curation, investigation, methodology, visualization, writing – original draft. Arij Ben Hassine: writing – review & editing. Pedro José Sanches Filho: data curation, investigation, methodology. M. Joana Neiva Correia: methodology, supervision, writing – review & editing. Pedro S. F. Mendes: conceptualization, methodology, supervision, writing – review & editing.

Conflicts of interest

There are no conflicts to declare.

Data availability

The raw and processed data for Fig. 2 and 3 are openly available in a FAIR format in Zenodo at https://doi.org/10.5281/zenodo.18313041. Details of data postprocessing are provided in section 1 of SI. Additional processed data supporting this study are included in supplementary information (SI).

Supplementary information: experimental section, review and analysis of oleic acid reaction pathways, Fig. S1–S15, Tables S1–S4, Eq. S1–S3 and additional references. See DOI: https://doi.org/10.1039/d6cy00118a.

Acknowledgements

The authors acknowledge funding from Fundação para a Ciência e Tecnologia (FCT) through CQE (UID/00100/2025; UID/PRR/00100/2025), IMS (LA/P/0056/2020) and CERENA (UID/04028/2025). Funding was also provided by the European Union (NextGenerationEU) through the Portuguese Government *via* the Agenda Moving2Neutrality no. C644927397-00000038, project no. 32. The authors also thank all the M2N project team for their insightful feedback.

Notes and references

† Across the literature, this conversion process is often described using different but overlapping terms, including hydroprocessing, hydroconversion, hydrotreatment or hydrodeoxygenation. To facilitate cross-disciplinary communication, in this work, hydroprocessing is employed and encompasses all hydrogen-assisted catalytic upgrading reactions in SAF production.
‡ Owing to the fast interconversion between fatty acids (*i.e.*, linoleic, oleic and stearic acids, see the previous section), fatty acid conversion was employed as a measurement of overall reaction extent for oleic acid deoxygenation.
§ All the mass fractions subsequently presented refer to the liquid organic phase in the C_{8+} fraction (vide SI, section 1.4), except when explicitly stated otherwise.

1 N. A. A. Qasem, A. Mourad and A. Abderrahmane, *et al.*, A recent review of aviation fuels and sustainable aviation fuels, *J. Therm. Anal. Calorim.*, 2024, **149**, 4287–4312, DOI: 10.1007/s10973-024-13027-5.
2 M. J. Watson, P. G. Machado and A. V. da Silva, *et al.*, Sustainable aviation fuel technologies, costs, emissions, policies, and markets: A critical review, *J. Cleaner Prod.*, 2024, **449**, 141472, DOI: 10.1016/j.jclepro.2024.141472.
3 A. M. Raji, B. Manescau and K. Chetehouna, *et al.*, Overview of combustion and emission characteristics of sustainable aviation fuels and standard JET A-1 fuel, *Fuel*, 2025, **402**, 136011, DOI: 10.1016/j.fuel.2025.136011.
4 B. Wang, Z. J. Ting and M. Zhao, Sustainable aviation fuels: Key opportunities and challenges in lowering carbon emissions for aviation industry, *Carbon Capture Sci. Technol.*, 2024, **13**, 100263, DOI: 10.1016/j.ccst.2024.100263.
5 A. Arias, C.-E. Nika and V. Vasilaki, *et al.*, Assessing the future prospects of emerging technologies for shipping and aviation biofuels: A critical review, *Renewable Sustainable Energy Rev.*, 2024, **197**, 114427, DOI: 10.1016/j.rser.2024.114427.
6 E. Borrill, S. C. L. Koh and R. Yuan, Review of technological developments and LCA applications on biobased SAF conversion processes, *Front. Fuel.*, 2024, **2**, 1397962, DOI: 10.3389/ffuel.2024.1397962.
7 M. Žula, M. Grilc and B. Likozar, Hydrocracking, hydrogenation and hydro-deoxygenation of fatty acids, esters

and glycerides: Mechanisms, kinetics and transport phenomena, *Chem. Eng. J.*, 2022, **444**, 136564, DOI: 10.1016/j.cej.2022.136564.

8 A. Kiméné, R. Wojcieszak and S. Paul, *et al.*, Catalytic decarboxylation of fatty acids to hydrocarbons over non-noble metal catalysts: the state of the art, *J. Chem. Technol. Biotechnol.*, 2019, **94**, 658–669, DOI: 10.1002/jctb.5776.

9 J. Weitkamp, Catalytic Hydrocracking—Mechanisms and Versatility of the Process, *ChemCatChem*, 2012, **4**, 292–306, DOI: 10.1002/cctc.201100315.

10 O. Calderon Rosales, L. Tao and Z. Abdullah, *et al.* Sustainable Aviation Fuel (SAF) State-of-Industry Report: State of SAF Production Process, 2024.

11 O. Kikhtyanin and D. Kubička, Understanding peculiarities in the simultaneous HDO and HDN during the hydroconversion of indole in its mixture with lauric acid and anisole over a NiMo/Al2O3catalyst – An important step towards efficient bio-oil upgrading, *Fuel*, 2026, **406**, 137144, DOI: 10.1016/j.fuel.2025.137144.

12 M. Song, X. Zhang and Y. Chen, *et al.*, Hydroprocessing of lipids: An effective production process for sustainable aviation fuel, *Energy*, 2023, **283**, 129107, DOI: 10.1016/j.energy.2023.129107.

13 P. Mäki-Arvela, M. Martínez-Klimov and D. Y. Murzin, Hydroconversion of fatty acids and vegetable oils for production of jet fuels, *Fuel*, 2021, **306**, 121673, DOI: 10.1016/j.fuel.2021.121673.

14 Z. Rahmawati, L. Santoso and A. McCue, *et al.*, Selectivity of reaction pathways for green diesel production towards biojet fuel applications, *RSC Adv.*, 2023, **13**, 13698–13714, DOI: 10.1039/d3ra02281a.

15 W. Jin, L. Pastor-Pérez and D. K. Shen, *et al.*, Catalytic Upgrading of Biomass Model Compounds: Novel Approaches and Lessons Learnt from Traditional Hydrodeoxygenation – a Review, *ChemCatChem*, 2019, **11**, 924–960, DOI: 10.1002/cctc.201801722.

16 X. Wang, Z. Zhang and Z. Yan, *et al.*, Catalysts with metal-acid dual sites for selective hydrodeoxygenation of lignin derivatives: Progress in regulation strategies and applications, *Appl. Catal., A*, 2023, **662**, 119266, DOI: 10.1016/j.apcata.2023.119266.

17 A. R. K. Gollakota, C. M. Shu and P. K. Sarangi, *et al.*, Catalytic hydrodeoxygenation of bio-oil and model compounds - Choice of catalysts, and mechanisms, *Renewable Sustainable Energy Rev.*, 2023, **187**, 113700, DOI: 10.1016/j.rser.2023.113700.

18 T. Vandevyvere, M. K. Sabbe and P. S. F. Mendes, *et al.*, NiCu-based catalysts for the low-temperature hydrodeoxygenation of anisole: Effect of the metal ratio on SiO2 and γ-Al2O3 supports, *Green Carbon*, 2023, **1**, 170–184, DOI: 10.1016/j.greenca.2023.10.001.

19 J. Poissonnier, C. Ranga and R. Lødeng, *et al.*, Oxygen functionality and chain length effects in HDO: Impact of competitive adsorption on reactivity, *Fuel*, 2022, **308**, 121940, DOI: 10.1016/j.fuel.2021.121940.

20 J. Gracia, A. Ayala-Cortés and C. Di Stasi, *et al.*, Highly selective catalytic hydrodeoxygenation of guaiacol to benzene in continuous operation mode, *Fuel Process. Technol.*, 2024, **255**, 108064, DOI: 10.1016/j.fuproc.2024.108064.

21 L. G. Moura, G. E. S. dos Santos and H. O. Alves, *et al.*, Hydrogenation of Guaiacol and Pyrolysis of Biomass Using Nickel and Niobium-Based Catalysts, *Catal. Lett.*, 2024, **154**, 2976–2988, DOI: 10.1007/s10562-023-04500-1.

22 Y. Han, A. P. P. Pires and M. Garcia-Perez, Co-hydrotreatment of the Bio-oil Lignin-Rich Fraction and Vegetable Oil, *Energy Fuels*, 2020, **34**, 516–529, DOI: 10.1021/acs.energyfuels.9b03344.

23 M. D. Denson, R. Manrique and M. Olarte, *et al.*, Co-hydrotreatment of Bio-oil and Waste Cooking Oil to Produce Transportation Fuels, *Energy Fuels*, 2024, **38**, 6982–6991, DOI: 10.1021/acs.energyfuels.3c05176.

24 O. Kikhtyanin, A. Smirnov and V. Korolova, *et al.*, Inhibiting effects during the co-conversion of lauric acid and anisole over Ni and NiMo catalysts, *Appl. Catal., A*, 2024, **685**, 119889, DOI: 10.1016/j.apcata.2024.119889.

25 B. Hočevar, M. Grilc and M. Huš, *et al.*, Mechanism, ab initio calculations and microkinetics of straight-chain alcohol, ether, ester, aldehyde and carboxylic acid hydrodeoxygenation over Ni-Mo catalyst, *Chem. Eng. J.*, 2019, **359**, 1339–1351, DOI: 10.1016/j.cej.2018.11.045.

26 B. Hočevar, M. Grilc and M. Huš, *et al.*, Mechanism, ab initio calculations and microkinetics of hydrogenation, hydrodeoxygenation, double bond migration and cis–trans isomerisation during hydrotreatment of C6 secondary alcohol species and ketones, *Appl. Catal., B*, 2017, **218**, 147–162, DOI: 10.1016/j.apcatb.2017.06.046.

27 M. Li, S. Xing and L. Yang, *et al.*, Nickel-loaded ZSM-5 catalysed hydrogenation of oleic acid: The game between acid sites and metal centres, *Appl. Catal., A*, 2019, **587**, 117112, DOI: 10.1016/j.apcata.2019.117112.

28 Z. Liu, J. Mei and X. Kong, *et al.*, Revealing the mechanism of selective hydrogenation of oleic acid on bifunctional hierarchical catalysts, *J. Catal.*, 2025, **450**, 116274, DOI: 10.1016/j.jcat.2025.116274.

29 O. Kikhtyanin and D. Kubička, Understanding the different deoxygenation reaction pathways of lauric acid over alumina-supported Ni and Co catalysts, *Sustainable Energy Fuels*, 2023, **7**, 485–501, DOI: 10.1039/D2SE01477G.

30 W. Song, Y. Liu and E. Baráth, *et al.*, Dehydration of 1-Octadecanol over H-BEA: A Combined Experimental and Computational Study, *ACS Catal.*, 2016, **6**, 878–889, DOI: 10.1021/acscatal.5b01217.

31 S. Sedtabute, T. Vitidsant and C. Ngamcharussrivichai, Production of jet fuel-range bio-hydrocarbons over nickel-based catalysts through hydrothermolysis without external H2: Effect of nanoporous supports, *Energy Convers. Manage.*, 2025, **331**, 119679, DOI: 10.1016/j.enconman.2025.119679.

32 N. Korica, P. S. F. Mendes and J. De Clercq, *et al.*, Interplay of Metal-Acid Balance and Methylcyclohexane Admixture Effect on n -Octane Hydroconversion over Pt/HUSY, *Ind. Eng.*

Chem. Res., 2021, **60**, 12505–12520, DOI: 10.1021/acs.iecr.1c01775.

33 C. Pfrang, M. Shiraiwa and U. Pöschl, Coupling aerosol surface and bulk chemistry with a kinetic double layer model (K2-SUB): oxidation of oleic acid by ozone, *Atmos. Chem. Phys.*, 2010, **10**, 4537–4557, DOI: 10.5194/acp-10-4537-2010.

34 R. Wang, C. Xia and B. Peng, Fundamental understanding and catalytic applications of hollow MFI-type zeolites, *Catal. Today*, 2022, **405–406**, 111–124, DOI: 10.1016/j.cattod.2022.06.026.

35 P. He, L. Li and Y. Shao, *et al.*, Recent Advances in Hydrodeoxygenation of Lignin-Derived Phenolics over Metal-Zeolite Bifunctional Catalysts, *ChemCatChem*, 2024, **16**, e202301681, DOI: 10.1002/cctc.202301681.

36 C. Abreu Teles, N. Duong and R. C. Rabelo-Neto, *et al.*, Evidence of dependence between the deoxygenation activity and metal–support interface, *Catal. Sci. Technol.*, 2022, **12**, 5961–5969, DOI: 10.1039/D2CY00969B.

37 E. Furimsky and F. E. Massoth, Deactivation of hydroprocessing catalysts, *Catal. Today*, 1999, **52**, 381–495, DOI: 10.1016/S0920-5861(99)00096-6.

38 P. Yan, M. Drewery and J. Mensah, *et al.*, Study on Catalyst Deactivation During the Hydrodeoxygenation of Model Compounds, *Top. Catal.*, 2020, **63**, 778–792, DOI: 10.1007/s11244-020-01310-2.

39 C. Abreu Teles, C. Ciotonea and A. Le Valant, *et al.*, Optimization of catalyst activity and stability in the m-cresol hydrodeoxygenation through Ni particle size control, *Appl. Catal., B*, 2023, **338**, 123030, DOI: 10.1016/j.apcatb.2023.123030.

40 M. Ogliaruso and J. Wolfe. *The synthesis of carboxylic acids and esters and their derivatives*, 1991, pp. 145–148. DOI: 10.1002/9780470772423.ch1.

41 N. J. Venditto, Y. S. Liang and R. K. El Mokadem, *et al.*, Ketone–Olefin Coupling of Aliphatic and Aromatic Carbonyls Catalyzed by Excited-State Acridine Radicals, *J. Am. Chem. Soc.*, 2022, **144**, 11888–11896, DOI: 10.1021/jacs.2c04822.

